Disruption of mouse poly(A) polymerase mGLD-2 does not alter polyadenylation status in oocytes and somatic cells

Tomoko Nakanishi [a, c], Satoshi Kumagai [a], Masanori Kimura [a], Hiromi Watanabe [a], Takayuki Sakurai [b], Minoru Kimura [b], Shin-ichi Kashiwabara [a] and Tadashi Baba [a]

[a] *Graduate School of Life and Environmental Sciences, University of Tsukuba, Tsukuba Science City, Ibaraki 305-8572, Japan*

[b] *School of Medicine, Tokai University , Japan*

[c] *Present address: Department of Molecular Biology, School of Life Science, Faculty of Medicine, Tottori University, Nishimachi 86, Yonago, Tottori 683-0853, Japan*

Abstract

The elongation of poly(A) tails in cytoplasm is essential for oogenesis and early embryogenesis in *Xenopus laevis*. mGLD-2 is a mouse homologue of *Xenopus* cytoplasmic poly(A) polymerase xGLD-2. We found an association of mGLD-2 with cytoplasmic polyadenylation components, CPEB and CPSF described in *Xenopus* oocytes. To clarify the role of mGLD-2 in mouse, we produced an mGLD-2 disrupted mouse line by homologous recombination. In spite of the ubiquitous expression of mGLD-2, the disrupted mice were apparently normal and healthy. Moreover, it was demonstrated that mGLD-2 disruption did not affect the poly(A) tail elongation in oocytes using reporter RNAs. Coincide with these observations, the maturation of the oocytes was normal and the mice were fertile. Thus mGLD-2 is dispensable for full-term development and oogenesis. Our results also indicate that there is another source of cytoplasmic poly(A) polymerase in mouse.

Keywords: mGLD-2, poly(A) polymerase, cytoplasmic polyadenylation, CPEB, CPSF, PABP, knockout mice, oocyte.

Introduction

The addition of mRNA poly(A) tails initially occurs in the eukaryotic nucleus. The processing of the mRNA precursors is one of the post-transcriptional gene regulations, because the length of the poly(A) tail is implicated in various aspects of mRNA metabolism, including the transport of mRNAs into the cytoplasm, mRNA stability, and translational control of mRNA [1]. However, the poly(A) tail is not exclusively added to mRNAs in the nucleus but also found to take place in the cytoplasm. The elongation of the poly(A) tail length in the cell cytoplasm are essential for normal gametogenesis [2-4] and early embryogenesis [5]. For example, meiotic maturation of *Xenopus* and mouse oocytes has been reported to require cytoplasmic polyadenylation of c-*mos* and cyclin B1 mRNAs for synthesis of the proteins [6, 7].

Several poly(A) polymerases responsible for the cytoplasmic polyadenylation are identified. Yeast Cid13 participates in DNA replication and genome maintenance, specifically targeting suc22 mRNA that encodes a subunit of ribonucleotide reductase [8], while yeast Cid1 and *C. elegans* GLD-2 targets a subset of mRNAs controlling the inhibition of mitosis and entry into meiosis [4, 9]. In mammals, we have reported that a testis specific cytoplasmic poly(A) polymerase, TPAP, elongates a poly(A) tail of mRNAs essential for spermatogenesis [3]. However, ploy(A) polymerases that may

function in somatic tissues are not known in mammals. Recently, we cloned the GLD-2 mouse homolog, mGLD-2, by PCR using cDNA prepared from an unfertilized mouse oocyte library as a template [10]. The mGLD-2 was expressed throughout the body and localized both in the nucleus and cytoplasm in somatic cells [10]. However, in oocytes in metaphase I and II stage after germinal vesicle breakdown, mGLD-2 was found exclusively in the cytoplasm [10]. mGLD-2 also possessed a CPE (cytoplasmic polyadenylation element)-specific polyadenylation activity in the ooplasm and a knockdown experiment caused the impairment of oogenesis [10]. Thus mGLD-2 was suggested to control the translation of specific proteins in oogenesis. In the present experiment, we produced an mGLD-2 gene disrupted mouse line to clarify the role of mGLD-2. Here, we report the effects of mGLD-2 on polyadenylation activity in somatic cells and oocytes together with the effects on live mouse including oogenesis.

Materials and methods

GST pull-down assay

Recombinant proteins were synthesized *in vitro* in the presence of ^{35}S-labeled Met (1000 Ci/mmol, MP biomedicals) by a TNT T7 Quick Coupled Transcription/Translation system (Promega). GST fusion proteins immobilized on

glutathione–Sepharose gel (Amersham Biosciences) were mixed with ^{35}S-labeled protein in 50 mM Tris/HCl, pH 7.5, containing 150 mM NaCl, 5 mM EDTA, 0.5% Nonidet P-40, and protease inhibitors for 1 h. After the gel was washed five times with the same buffer, proteins on the gel were treated with a Laemmli buffer, and analyzed by SDS–PAGE.

Generation of mutant mice lacking mGLD-2

Genomic clones encoding mGLD-2 were isolated from a mouse 129/SvJ genomic DNA library in λFIXII (Stratagene) using ^{32}P-labeled DNA fragments as probes. Of the ten clones isolated, a clone, termed MGLD4, was used for construction of a targeting vector carrying a neomycin-resistance (*neo*) expression cassette flanked by a 1.5- and 9.7-kbp genomic region of *mGLD-2*. For negative selection, an *HSV-TK* (*tk*) cassette was inserted at the 5'-end of the targeting vector (Fig. 1C). The construct was designed to replace a part of second exon and the whole third exon with the *neo* expression cassette. Following electroporation of the targeting vector into D3 mouse ES cells, homologous recombinants were selected by using G418 and gancyclovir. Ten ES cell clones containing the targeted mutation were selected from 186 clones, and injected into C57BL/6 mouse blastocysts. Chimeric male mice were crossed to

C57BL/6 females (SLC Inc., Japan) to establish the heterozygous mutant lines. All animal experiments were carried out according to the Guide for the Care and Use of Laboratory Animals in the University of Tsukuba.

Blot hybridization

Genomic DNA was prepared from the mouse tail, digested by *Bgl*II and *Pst*I, separated by agarose gel electrophoresis, and transferred onto Hybond-N^+ nylon membranes (Amersham Biosciences). Total cellular RNA was prepared from liver using Isogen (Nippon Gene, Japan) [3]. The RNA samples were glyoxylated, separated by agarose gel electrophoresis, and transferred onto the nylon membranes. The blots were probed by ^{32}P-labeled DNA fragments, and analyzed by a BAS-1800II Bio-Image Analyzer (Fuji Photo Film, Japan).

Antibodies and immunoblot analysis

Affinity-purified anti-mGLD-2 antibody was prepared as described previously [10]. The antibody against β-tubulin was purchased from Sigma. Mouse tissues were homogenized at 4°C in 20 mM HEPES/KOH, pH 7.5, containing 150 mM NaCl, 1 mM EDTA, 1.0% Triton X-100, 0.5% deoxycholate, 0.1% SDS. Oocytes were lysed at

4°C in 10 mM Tris/HCl, pH 8.0, containing 1.5 mM $MgCl_2$, 10 mM KCl, 1.0% Triton X-100, 0.5% deoxycholate, 0.1% SDS. Proteins in the supernatant solution were subjected to Western blot analysis. The immunoreactive proteins were visualized by an ECL Western blotting detection kit (Amersham Biosciences).

Immunoprecipitation

Nuclear extract of mouse liver was prepared as previously described [10]. Protein A-agarose beads (50% slurry, Pierce), bound with the affinity purified anti-mGLD-2 antibody, were mixed with the nuclear extracts (0.5 mg protein), and then incubated at 4°C overnight. After centrifugation, the pellet was washed five times with the binding buffer, and then subjected to the measurement of polyadenylation activity.

Assay of polyadenylation activity

Poly(A) polymerase activities were determined by measuring incorporation of AMP from [α-^{32}P]ATP (400 Ci/mmol, MP biomedicals) into oligo$(A)_{12}$ RNA primer in the presence of $MnCl_2$ [10]. The reaction mixtures were sequentially spotted onto Whatman DE-81 paper, washed with 0.1 M phosphate buffer, pH 7.0, and then measured by liquid scintillation counting.

Polymerase chain reaction (PCR)

Total cellular RNAs were extracted from metaphase II-arrested oocytes using Isogen (Nippon Gene) [10]. For RT-PCR, first-strand cDNA was synthesized from total RNAs by a SuperScript III reverse transcriptase (Invitrogen) using oligo dT_{20} as a primer. A portion of the synthesized cDNAs was subjected to PCR using specific primer sets. A set of primers, 5'-TCGGCCCTTCGGCGTGGACG-3' (sense) and 5'-TGTAAGGACACAGCTCTAGAC-3' (antisense), corresponding to the sequences in the first and third exons of *mGLD-2*, respectively, was used for assessment of the third exon replacement by *neo*. For the PCR-based poly(A) test, total RNA from oocytes were ligated to a 32-mer RNA oligonucleotide, 5'-UACGCAUCAUACGCUGUGGCGUACCUUGUA-3' (60 pmol), and reacted at 42°C for 50 min with SuperScript II reverse transcriptase (Invitrogen), using a PAT1 oligonucleotide, 5'-ACAAGGTACGCCACAGCGTATG-3', as a primer. A portion of the reaction mixture was subjected to first round PCR using a set of PAT1 and a gene-specific primer. Second round PCR was carried out using a nested set of primers, PAT2, 5'-GGCTCGAGGTACGCCACAGCGTATGATG-3', and another gene-specific primer. Details of the PCR conditions, including other primer sequences are described

previously [10].

RNA synthesis in vitro

DNA fragments including the CPE/HEX and mutCPE/HEX of cyclin B1 mRNA were amplified by PCR from a mouse testis cDNA library [11] using primer sets, CYBP7/9 and CYBP8/9, respectively. The following oligonucleotides were used as primers: CYBP7 (5'–AAGTCGACTTTTAATTTATACATCTGATATCAAG–3'), CYBP8 (5'–AAGTCGACTTTGGATTTATACATCTGATATCAAG–3'), and CYBP9 (5'–TAAAGCTTTCCACCAATAAATTTTATTCAA–3'). The PCR products were introduced between EGFP and 45 adenosine residues of a pEGFPA45 vector. The resulting plasmids were linearized by cutting with *Bsm*BI. RNAs were synthesized with T3 polymerase using an mMESSAGE mMACHINE T3 Kit (Ambion).

Microinjection

Oocytes at metaphase II stage were collected from the oviducts of female mice that had been superovulated by pregnant mare's serum gonadotropin (5 units, ASKA Pharmaceutical, Japan) followed by human chorionic gonadotropin (5 units, ASKA Pharmaceutical) 48 h later. A mixture of equal volumes of RNAs (1 mg/ml) and

157 TRITC-labeled dextran (50 μM) was injected into the oocytes using a Piezo-driven
158 micromanipulator (Prime Tech Ltd., Japan). Approximately 10 pl of the RNA solution
159 was introduced into the oocytes. The oocytes were incubated in drops of kSOM
160 medium [10] covered with mineral oil (Sigma) at 37°C under 5% CO_2 in air. The
161 oocytes were observed using an Olympus IX-70 inverted microscope equipped with a
162 SPOT RT camera (Diagnostic Instruments). The 16-bit digital images were analyzed
163 by using a Metamorph software (Universal Imaging Corp.).
164
165 **Results and discussion**
166 ***Interaction of mGLD-2 with the cytoplasmic polyadenylation complex***
167 GLD-2 in *C. elegans* encodes the catalytic moiety of a cytoplasmic poly(A)
168 polymerase (PAP) that is associated with a regulation of mitosis/meiosis decision and
169 other germline events [4]. xGLD-2 from *Xenopus* is also known to function in
170 ooplasm which implies that cytoplasmic PAPs are fundamental factors to regulate the
171 translation of mRNA [12]. The most prominent and well investigated site for
172 cytoplasmic polyadenylation is the oocytes. In *Xenopus*, the translational levels of the
173 mRNAs are controlled by xGLD-2 together with polyadenylation regulatory factors
174 such as CPEB (CPE-binding protein) and CPSF (cleavage and specificity factor)

during oogenesis and early embryogenesis [12]. We have already shown the CPE (cytoplasmic polyadenylation element)-specific polyadenylation activity of mGLD-2 [10]. To further investigate the roles of mGLD-2 *in vitro*, we produced recombinant mGLD-2 and examined its association with various GST-tagged proteins included in cytoplasmic polyadenylation machinery. As shown in Fig. 1A, mouse CPEB1 [13] and cytoplasmic poly(A) binding protein 1, PABPC1 [14], interacted with mGLD-2. CPEB2 [15], which is expressed in mouse testis was also found to interact with mGLD-2. To analyze the binding ability of mouse CPSF160 [16], a subunit of CPSF, to mGLD-2, we produced GST-tagged mutant mGLD-2 (D215A), which has almost no polyadenylation activity [10], and mixed it with recombinant CPSF160 (Fig. 1B). This was necessary due to the low yield of GST-tagged CPSF160 and mGLD-2. Moreover, the association of recombinant CPEB1, CPEB2, and PABPC1 with GST-tagged D215A was also demonstrated (Fig. 1B). These data indicate the involvement of mGLD-2 in the regulation of mRNA translation by associating with the cytoplasmic polyadenylation complex which is formed on the poly(A) tail.

Production of mGLD-2-deficient mice

Mutant mice lacking mGLD-2 were produced by homologous recombination in ES

193 cells, using a targeting vector containing *neo* and *tk* expression cassettes (Fig. 1C). A
194 part of the second exon and the whole third exon were replaced by the *neo* cassette.
195 The genotypes of wild-type (*mGLD-2*$^{+/+}$), heterozygous (*mGLD-2*$^{+/-}$), and homozygous
196 (*mGLD-2*$^{-/-}$) mice for the null mutation of *mGLD-2* were identified by Southern blot
197 analysis of genomic DNA (Fig. 1D). Mating of *mGLD-2*$^{+/-}$ male and female mice
198 yielded the expected Mendelian frequency of *mGLD-2*$^{-/-}$ mice (*mGLD-2*$^{+/+}$: *mGLD-2*$^{+/-}$:
199 *mGLD-2*$^{-/-}$ = 10 (17%) : 34 (58%) : 15 (25%) for 59 offspring from 6 litters). Both
200 *mGLD-2*$^{-/-}$ males and females were apparently normal in behavior, body size, and health
201 condition. Northern blot analysis indicated the absence of mGLD-2 mRNA in the
202 liver of *mGLD-2*$^{-/-}$ mice (Fig. 1E). Moreover, protein extracts of the *mGLD-2*$^{-/-}$ liver
203 completely lacked mGLD-2 (Fig. 1F). These data demonstrate the successful gene
204 disruption of *mGLD-2*$^{-/-}$ in our mutant mouse line.
205
206 ***Analysis of mGLD-2-deficient somatic cells***
207 mGLD-2 localizes both in the nucleus and in the cytoplasm [10]. We prepared
208 mGLD-2 from the nuclear extract of mouse liver cells by immunoprecipitation and
209 assayed the polyadenylation activity. As a result, it was demonstrated the
210 polyadenylation activity in *mGLD-2*$^{+/-}$ mice are about half that of the *mGLD-2*$^{+/+}$ mice

211 and disappeared in *mGLD-2*$^{-/-}$ mice (Fig. 2A). However, when we observed the total
212 polyadenylation activity using nuclear or cytoplasmic extract, we could not find any
213 significant differences between *mGLD-2*$^{+/-}$ and *mGLD-2*$^{-/-}$ mouse extracts (Fig. 2B).
214 The results indicate that the disruption of mGLD-2 did not affect the overall poly(A)
215 length in the liver.
216
217 ***Analysis of mGLD-2-deficient oocytes***
218 We previously reported that over expression of mGLD-2 in mouse oocytes could
219 selectively elongate the poly(A) tail length of cyclin B1 and Mos mRNAs [10]. This
220 may indicate that mGLD-2 is involved in oogenesis by controlling the translation of key
221 factors. Thus we next examined the effect of mGLD-2 disruption on oocytes.
222 Naturally, the expression of mGLD-2 was demonstrated to disappear totally in
223 *mGLD-2*$^{-/-}$ mouse oocytes in mRNA and also in protein levels (Figs. 3A and 3B).
224 However, as observed in the liver, no significant decrease in overall polyadenylation
225 activity was evident in *mGLD-2*$^{-/-}$ mouse oocytes (Fig. 3C). For more detailed analysis,
226 we examined the change in poly(A) tail length of cyclin B1 and Mos mRNA by
227 amplifying the poly(A) tails by PCR using two primer sets described in the materials
228 and methods. However, we could not find any significant difference in the poly(A)

229 tails in germinal vesicle, metaphase I and metaphase II-stage oocytes from *mGLD-2*$^{-/-}$
230 mice (Fig. 3D).
231
232 ***Noninvasive measurement of the cytoplasmic polyadenylation activity***
233 In order to quantify the CPE dependent polyadenylation activity in oocytes, we
234 produced synthetic EGFP RNA with 3'-UTR of cyclin B1 which contained CPE and
235 AAUAAA followed by a 45 bp length poly(A) tail (Fig. 4A). Since, the elongation of
236 cyclin B1 poly(A) tail is reported to take place in metaphase I and II-stage oocytes [7],
237 we injected the reporter RNA into oocytes at metaphase II stage. Six hours after the
238 introduction of the RNA, a tremendous increase of fluorescence from EGFP was
239 observed (Fig. 4B). On the other hand, the oocytes did not become fluorescent when
240 the reporter RNA which contained mutated CPE was injected (Figs. 4A and 4B).
241 Using this system, we measured the cytoplasmic polyadenylation activity in mGLD-2
242 disrupted oocytes. Different from our expectation, as shown in Figs. 4B and 4D, the
243 mGLD-2 null oocytes became fluorescent by the injection of the reporter RNA.
244 Concomitant with this observation, the elongation of the poly(A) tail was observed in
245 the reporter RNA including the CPE sequence (Fig. 4C). Reflecting the normal
246 cytoplasmic polyadenylation in mGLD-2 knockout mouse oocytes, the transition rate of

247 *mGLD-2*$^{-/-}$ mouse oocytes from germinal vesicle to metaphase II stage *in vitro* was
248 comparable to that of *mGLD-2*$^{+/-}$ oocytes (+/–,80 ± 13%, n = 3; –/–,77 ± 11%, n = 3).
249 Moreover, the spindle formation in the mGLD-2 disrupted oocytes was normal when
250 oocytes were observed after staining with anti-β-tubulin antibody and Hoechst 33342
251 (data not shown). The lack of apparent phenotype was reassured by the normal
252 number of pups obtained from *mGLD-2*$^{-/-}$ female mice (7.9 ± 3.0, n = 13) compared to
253 the *mGLD-2*$^{+/-}$ female mice (8.9 ± 2.7, n = 8) when mated with wild-type mice.
254
255 In *Xenopus*, there is a notion that xGLD-2 is the responsible enzyme for
256 CPE-dependent cytoplasmic polyadenylation, but this was not applicable in mouse since
257 mGLD-2 was indicated not to be an exclusive enzyme for the polyadenylation. In
258 mammalian cells, six PAPs have been identified: canonical PAP (PAPI and PAPII) [17],
259 TPAP [3], neo-PAP [18], PAPγ [19], GLD-2 [4], and nuclear-encoded mitochondrial
260 PAP, mitoPAP [20]. These mammalian PAPs, except TPAP, GLD-2, and mitoPAP, are
261 exclusively localized in the nucleus. Nuclear PAP localizes in the cytoplasm during
262 metaphase where the nuclear envelope disappears. However, canonical PAP has been
263 reported to be inactivated via phosphorylation by p34cdc2/cyclinB complex during
264 metaphase [21]. Mitochondria is another source of PAP, but mitoPAP localizes only

inside the mitochondria [20]. Thus PAP that functions in cytoplasm is not known in mouse except mGLD-2. The result of our RNAi experiment suggested an important role of mGLD-2 in mouse oocyte maturation [10]. Contrary to our expectation, we could not find any phenotype in mGLD-2 deficient mice. This might be a result of some compensation effect (up regulation) of a yet unknown mouse cytoplasmic poly(A) polymerase. However, the compensation was not effectively functional in the RNAi experiment [10], which may relate to the nature of the sudden impairment of mGLD-2 activity in RNAi.

Combining the results from other cases, where distinctive phenotypes are observed such as disruption of GLD-2 in *C. elegans*, Cid1 and Cid13 in yeast, [4, 8, 9, 22] and testis specific PAP (TPAP) in mouse [3], the lack of phenotype in the mGLD-2 disrupted mouse line may indicate the existence of a yet unknown cytoplasmic PAP. We presume that it would be worth to quest a new cytoplasmic PAP to elucidate the regulation of mRNA translation leading to dramatize various characteristics of living cells.

Acknowledgments

This study was supported by Japan Society for the Promotion of Science (JSPS) and

283 Ministry of Education, Culture, Sports, Science and Technology in Japan (MEXT);
284 grant numbers: 15208033, 17700376, 18208029, 18058005.

References

[1] M. Wickens, P. Anderson, R.J. Jackson, Life and death in the cytoplasm: messages from the 3' end, Curr. Opin. Genet. Dev. 7 (1997) 220-232.

[2] J. Tay, J.D. Richter, Germ cell differentiation and synaptonemal complex formation are disrupted in CPEB knockout mice, Dev. Cell 1 (2001) 201-213.

[3] S. Kashiwabara, J. Noguchi, T. Zhuang, K. Ohmura, A. Honda, S. Sugiura, K. Miyamoto, S. Takahashi, K. Inoue, A. Ogura, T. Baba, Regulation of spermatogenesis by testis-specific, cytoplasmic poly(A) polymerase TPAP, Science 298 (2002) 1999-2002.

[4] L. Wang, C.R. Eckmann, L.C. Kadyk, M. Wickens, J. Kimble, A regulatory cytoplasmic poly(A) polymerase in Caenorhabditis elegans, Nature 419 (2002) 312-316.

[5] J.D. Richter, Cytoplasmic polyadenylation in development and beyond, Microbiol. Mol. Biol. Rev. 63 (1999) 446-456.

[6] M.D. Sheets, M. Wu, M. Wickens, Polyadenylation of c-mos mRNA as a control point in Xenopus meiotic maturation, Nature 374 (1995) 511-516.

[7] J. Tay, R. Hodgman, and J. D. Richter, The control of cyclin B1 mRNA translation during mouse oocyte maturation, Dev. Biol. 221 (2000) 1-9.

[8] S. Saitoh, A. Chabes, W.H. McDonald, L. Thelander, J.R. Yates, P. Russell,

303 Cid13 is a cytoplasmic poly(A) polymerase that regulates ribonucleotide reductase
304 mRNA, Cell 109 (2002) 563-573.
305 [9] R.L. Read, R.G. Martinho, S.W. Wang, A.M. Carr, C.J. Norbury, Cytoplasmic
306 poly(A) polymerases mediate cellular responses to S phase arrest, Proc. Natl. Acad. Sci.
307 USA 99 (2002) 12079-12084.
308 [10] T. Nakanishi, H. Kubota, N. Ishibashi, S. Kumagai, H. Watanabe, M. Yamashita,
309 S. Kashiwabara, K. Miyado, T. Baba, Possible role of mouse poly(A) polymerase
310 mGLD-2 during oocyte maturation, Dev. Biol. 289 (2006) 115-126.
311 [11] S. Kashiwabara, T. Baba, M. Takada, K. Watanabe, Y. Yano, and Y. Arai,
312 Primary structure of mouse proacrosin deduced from the cDNA sequence and its gene
313 expression during spermatogenesis, J. Biochem. (Tokyo) 108 (1990) 785-791.
314 [12] J.D. Richter, CPEB: a life in translation, Trends Biochem. Sci. 32 (2007)
315 279-285.
316 [13] R. Mendez, J.D. Richter, Translational control by CPEB: a means to the end,
317 Nat. Rev. Mol. Cell Biol. 2 (2001) 521-529.
318 [14] D.A. Mangus, M.C. Evans, A. Jacobson, Poly(A)-binding proteins:
319 multifunctional scaffolds for the post-transcriptional control of gene expression,
320 Genome Biol. 4 (2003) 223.

[15] Y. Kurihara, M. Tokuriki, R. Myojin, T. Hori, A. Kuroiwa, Y. Matsuda, T. Sakurai, M. Kimura, N. B. Hecht, S. Uesugi, CPEB2, a novel putative translational regulator in mouse haploid germ cells, Biol. Reprod. 69 (2003) 261-268.

[16] B. Dass, E.N. Attaya, A. Michelle Wallace, C.C. MacDonald, Overexpression of the CstF-64 and CPSF-160 polyadenylation protein messenger RNAs in mouse male germ cells, Biol. Reprod. 64 (2001) 1722-1729.

[17] W. Zhao, J.L. Manley, Complex alternative RNA processing generates an unexpected diversity of poly(A) polymerase isoforms, Mol. Cell. Biol. 16 (1996) 2378-2386.

[18] S.L. Topalian, S. Kaneko, M.I. Gonzales, G.L. Bond, Y. Ward, J.L. Manley, Identification and functional characterization of neo-poly(A) polymerase, an RNA processing enzyme overexpressed in human tumors, Mol. Cell. Biol. 21 (2001) 5614-5623.

[19] C.B. Kyriakopoulou, H. Nordvarg, A. Virtanen, A novel nuclear human poly(A) polymerase (PAP), PAP gamma, J. Biol. Chem. 276 (2001) 33504-33511.

[20] R. Tomecki, A. Dmochowska, K. Gewartowski, A. Dziembowski, P.P. Stepien, Identification of a novel human nuclear-encoded mitochondrial poly(A) polymerase, Nucleic Acids Res. 32 (2004) 6001-6014.

[21] G.L. Bond, C. Prives, J.L. Manley, Poly(A) polymerase phosphorylation is dependent on novel interactions with cyclins, Mol. Cell. Biol. 20 (2000) 5310-5320.

[22] S.W. Wang, T. Toda, R. MacCallum, A.L. Harris, C. Norbury, Cid1, a fission yeast protein required for S-M checkpoint control when DNA polymerase delta or epsilon is inactivated, Mol. Cell. Biol. 20 (2000) 3234-3244.

Figure Legend

Figure 1

Direct interaction of mGLD-2 with components in polyadenylation complex and generation of mGLD-2-deficient mice. (A) GST pull-down assays were carried out using ^{35}S-labeled mGLD-2 and each polyadenylation components fused with GST. (B) GST pull-down assays were carried out using ^{35}S-labeled polyadenylation components and mutant mGLD-2, D215A, fused with GST. (C) Schematic representation of the gene targeting strategy. For detail, refer to the materials and methods. Restriction enzyme sites indicated are as follows: S, *Sac*I; G, *Bgl*II; P, *Pst*I; X, *Xho*I, Sa; *Sal*I. (D) Southern blot analysis of genomic DNA from wild-type (*mGLD-2*$^{+/+}$, +/+), heterozygous (*mGLD-2*$^{+/-}$, +/–) and homozygous (*mGLD-2*$^{-/-}$, –/–) mice. Genomic DNA was digested by *Bgl*II and *Pst*I, separated by agarose gel electrophoresis, and subjected to Southern blot analysis using a ^{32}P-labeled DNA fragment (S-probe in panel C) as a probe. The wild-type and targeted alleles yielded 4.7- and 5.5-kbp DNA bands, respectively. (E) Northern blot analysis of total RNAs from liver tissues. Two forms (3.5 and 2.3 kbp) of mGLD-2 mRNA, distinguished by the length of the 3'-untranslated region encoded by the same exon of the mGLD-2 gene, were absent in *mGLD-2*$^{-/-}$ mouse liver. G3PDH, glyceraldehyde-3-phosphate

362 dehydrogenase. (F) Western blot analysis of protein extracts from liver tissues.
363 Proteins (10 μg) were loaded in each lane and probed with affinity-purified
364 anti-mGLD-2 or anti-β-tubulin antibody. The *mGLD-2*$^{-/-}$ mouse liver lacked mGLD-2
365 with the size of 54 kDa. An asterisk indicates the location of a 51-kDa protein
366 nonspecifically immunoreactive with the anti-mGLD-2 antibody.

367

368 ***Figure 2***

369 Polyadenylation activity in *mGLD-2*$^{-/-}$ mouse liver. (A) Enzyme activity of
370 mGLD-2 in the liver nuclear extract. Nuclear protein (0.5 mg) of *mGLD-2*$^{+/+}$ (open
371 circle), *mGLD-2*$^{+/-}$ (shaded circle), and *mGLD-2*$^{-/-}$ (closed circle) mice were
372 immunoprecipitated using affinity-purified anti-mGLD-2. Polyadenylation activities
373 of the precipitation were monitored by measuring the incorporation of AMP from
374 [α-^{32}P]ATP into oligo(A)$_{12}$ primer. (B) Total polyadenylation activity of nuclear and
375 cytoplasmic protein (4 μg) extracted from *mGLD-2*$^{+/-}$ (shaded column) and *mGLD-2*$^{-/-}$
376 (closed column) mouse liver. Relative activities measured at 6 h are indicated as
377 means ± S.D., where $n = 3$.

378

379 ***Figure 3***

Polyadenylation activity in *mGLD-2*$^{-/-}$ mouse oocytes. (A) RT-PCR analysis of total RNAs from metaphase II-stage oocytes. No DNA band was detected in *mGLD-2*$^{-/-}$ mice. G3PDH, glyceraldehyde-3-phosphate dehydrogenase. (B) Western blot analysis of protein extracts from metaphase II-stage oocytes. Proteins of oocytes (50 cells per lane) were loaded in each lane and probed with affinity-purified anti-mGLD-2 or anti-β-tubulin antibody. (C) Total polyadenylation activity of protein extracts (50 cells) from metaphase II-stage oocytes of *mGLD-2*$^{+/-}$ (shaded column) and *mGLD-2*$^{-/-}$ (closed column) mice. Relative activities measured at 6 h are indicated as means ± S.D., where $n = 4$. (D) The sizes of poly(A) tails of cyclin B1, Mos, and β-actin, as a negative control. Total RNAs from the GV-, MI- and MII-stage oocytes (50 cells) of *mGLD-2*$^{+/-}$ and *mGLD-2*$^{-/-}$ mouse were subjected to PCR-based poly(A) test.

Figure 4

Cytoplasmic polyadenylation activity of *mGLD-2*$^{-/-}$ mouse oocytes. (A) Schematic representation of the synthetic reporter RNAs. EGFP open reading frame was fused to 48 bp of the cyclin B1 3'-UTR. The polyadenylation hexanucleotide (AAUAAA), CPE and poly(A) tail are indicated. (B) Fluorescence images of *mGLD-2*$^{+/-}$ and

398 *mGLD-2*$^{-/-}$ mouse oocytes 6 h after the injection of the reporter RNAs. TRITC-labeled
399 dextran was coinjected with the RNA to normalize the amount of RNA injected (D).
400 Scale bar = 100 μm. (C) PCR-based poly(A) test of reporter RNAs injected into
401 *mGLD-2*$^{+/-}$ and *mGLD-2*$^{-/-}$ mouse oocytes. Oocytes (8 cells) were subjected to the
402 analysis 6 h after the RNA injection. (D) Quantification of cytoplasmic
403 polyadenylation activities of *mGLD-2*$^{+/-}$ and *mGLD-2*$^{-/-}$ mouse oocytes. EGFP
404 fluorescence of the oocytes was measured at 2-h intervals, and was divided by that of
405 the TRITC-labeled dextran coinjected with the reporter RNA. The highest intensity of
406 an oocyte after 6-h incubation was set at 100%. Number of *mGLD-2*$^{+/-}$ oocytes
407 examined: 15 (n = 2) and 8 (n = 1) injected with CPE(-) and CPE(+) RNA, respectively.
408 Number of *mGLD-2*$^{-/-}$ oocytes examined: 17 (n = 2) and 10 (n = 1) injected with CPE(-)
409 and CPE(+) RNA, respectively. The data indicate the means ± S.D.
410

Figure 1. Nakanishi *et al.*

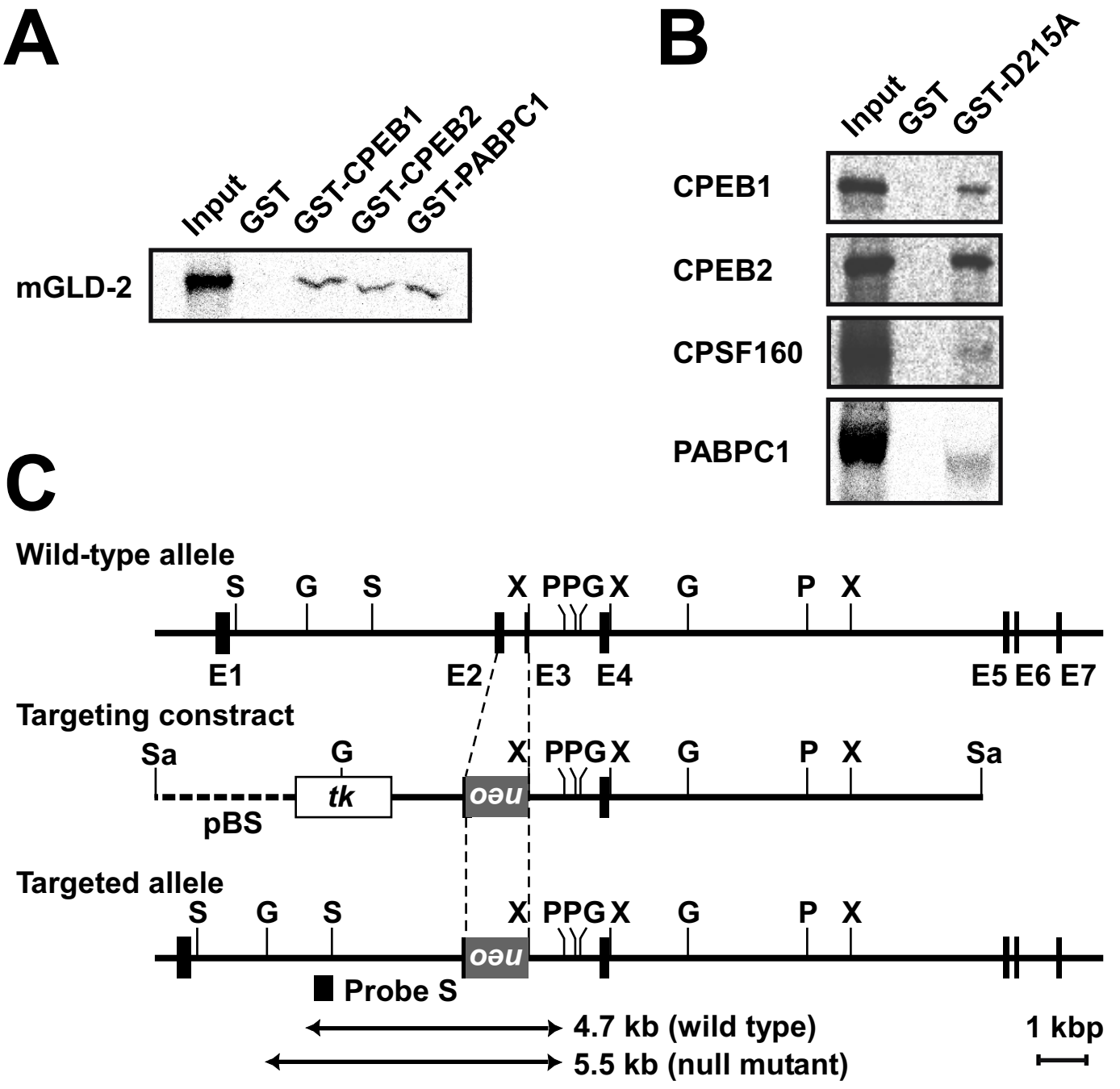

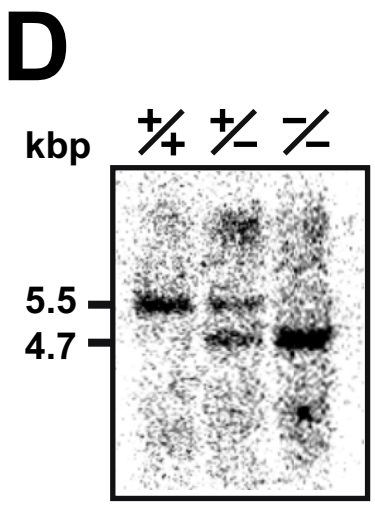

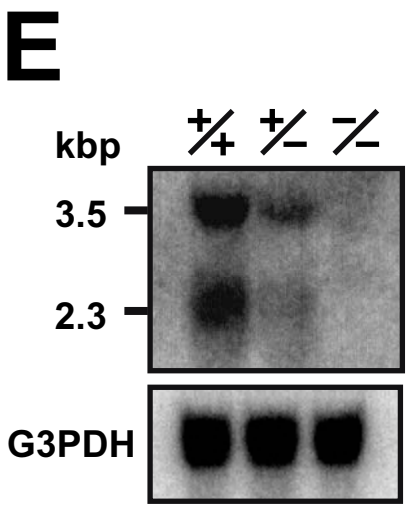

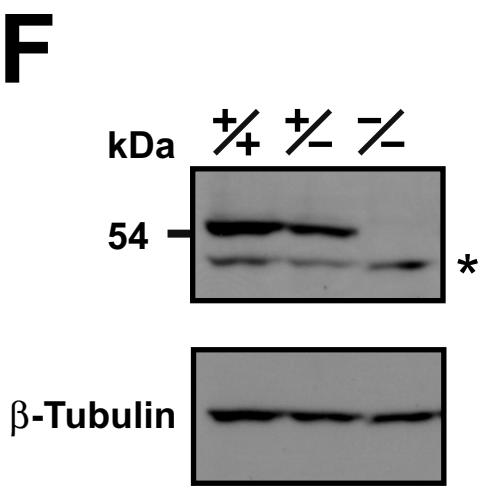

Figure 2. Nakanishi *et al.*

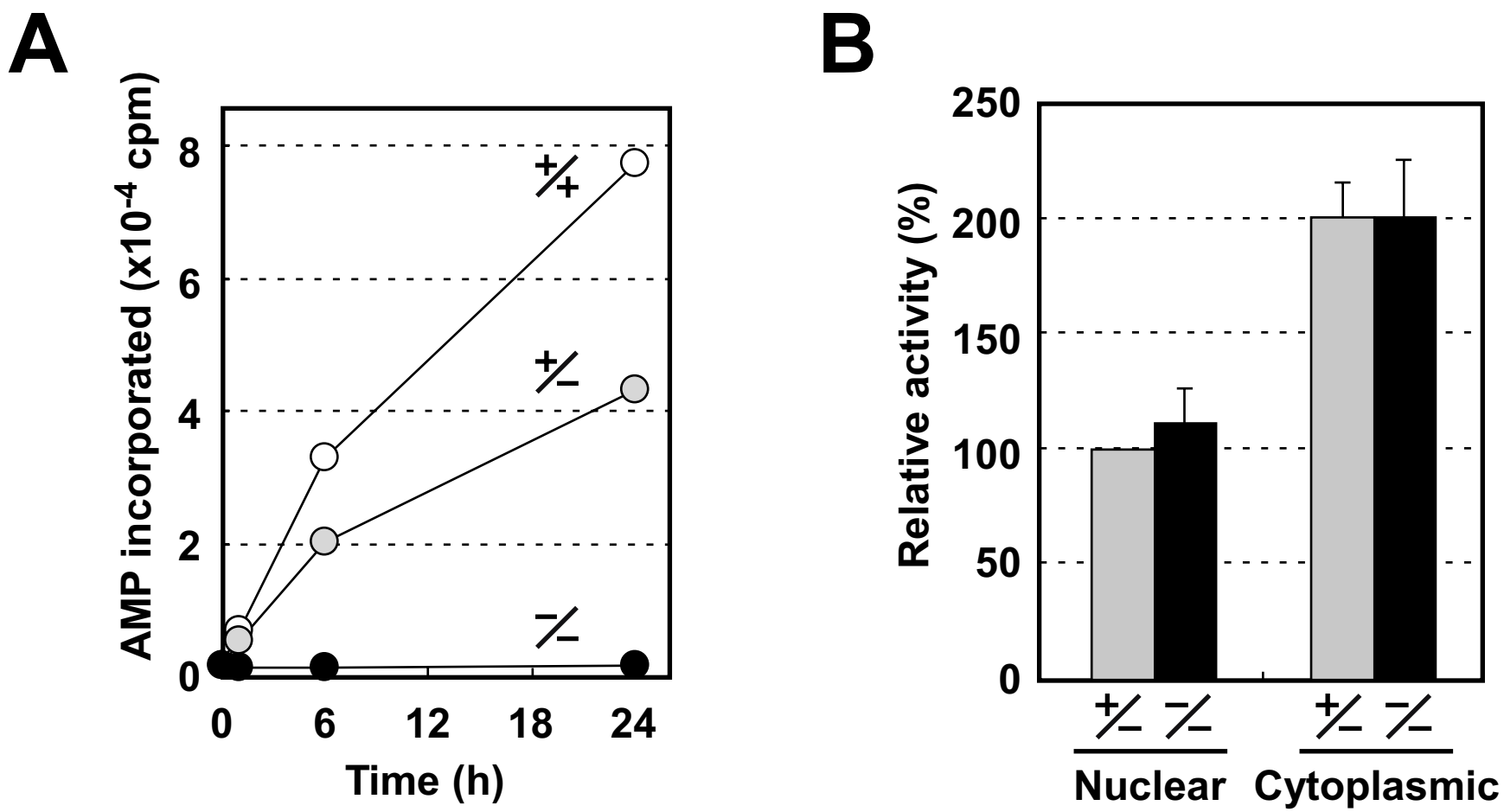

Figure 3. Nakanishi *et al.*

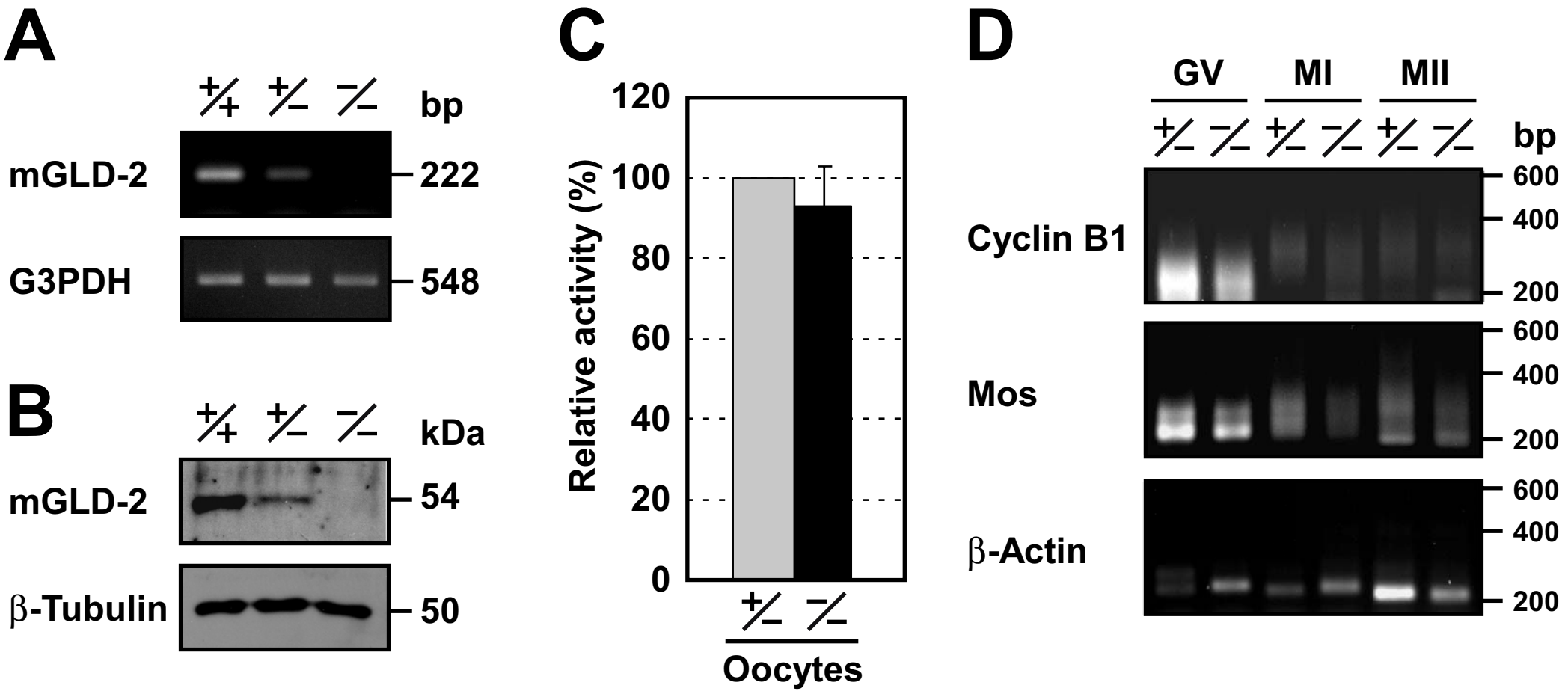

Figure 4. Nakanishi *et al.*